Application of Image Processing in Soil Mechanics

Luke Knodel

A Senior Thesis submitted in partial fulfillment
of the requirements for graduation
in the Honors Program
Liberty University
Spring 2023

Acceptance of Senior Honors Thesis
This Senior Honors Thesis is accepted in partial
fulfillment of the requirements for graduation from the
Honors Program of Liberty University.

_____
Kalehiwot Manahiloh, Ph.D.
Thesis Chair

_____
John Vadnal, Ph.D.
Committee Member

_____
David Schweitzer, Ph.D.
Assistant Honors Director

_____
Date

ACKNOWLEDGMENTS

I want to thank my God for giving life purpose throughout my academic career and I want to thank Dr. Manahiloh for his teachings and guidance in the thesis writing process. In addition, I would like to thank my parents for encouraging me during my schooling years and being supportive of my work in the Liberty University Honor's Program.

TABLE OF CONTENTS

ABSTRACT

Whenever someone digs a hole in the ground or takes a relaxing walk on the beach, they directly interact with the soil. In its basic form, soil consists of solid, water, and air phases. Unlike water and metals, soil is a particulate media, and the relative proportion of the individual phases significantly influences its physical properties. Various studies have analyzed soil using image processing to determine its morphological properties. Research involving the digital processing of X-ray Computed Tomography (X-ray CT) images of soil to retrieve physically meaningful information is gaining recognition. This study investigates two-dimensional X-ray CT images of unsaturated granular media taken at specific locations on the wetting and drying curves of the soil water characteristic curve (SWCC) determined for the granular media. The images are segmented into three distinct phases of the media through image histogram-based thresholding. The porosity, void ratio, and degree of saturation are evaluated by counting the appropriate pixels for each phase and applying calibrations between pixels and physical dimensions.

Chapter 1

INTRODUCTION

1.1 Introduction

What is the first thing someone does when they break a bone or suffer a significant injury? First, they would probably shout in pain. Second, they would wonder if they fractured a bone, and third, they would plan to get an X-ray as soon as possible. What if there were a way to use X-ray technology to examine soil samples to recognize their physical makeup? In its general state, soil comprises air, water, and solid phases. The relative proportion of each phase influences how soil behaves. Flow, compressibility, and strength-related properties of soils are governed by how the three phases interact. When a soil sample is loaded, it deforms and fails by shear. Soil specimens that fail in shear could barrel or form a shear band. A typical shear testing procedure involves taking samples to a lab for testing that may take days. In addition, such methods of investigation are destructive. Image processing has been a non-destructive and accurate method for analyzing soil samples for the past 20 years.

1.2 Objective and Scope

This thesis emphasizes the extent of the application of digital image processing and X-ray Computed Tomography (X-ray CT) in Geosciences. Digital images obtained from X-ray CT will be analyzed using the image processing tool of Image-Pro Premier®.

1.3 Thesis Organization

Chapter 1 – Introduces the thesis topic, objective and scope, and the thesis organization.

Chapter 2 – Reviews past research covering the topics of soil analysis using image processing methods and algorithms. The studies range from 2D photos of specimens to complete 3D models built from CT scanned image stacks.

Chapter 3 – Builds upon the reviewed literature, discusses the application of soil image processing and segmentation. The methods used are described in detail.

Chapter 4 – Results are calculated in depth and presented in tables.

Chapter 5 – References are listed for the thesis in APA formatting.

Chapter 2

LITERATURE REVIEW

2.1 Applications of Image processing

Image processing methods have been used in many research studies involving soil analysis. Applications range from photogrammetry of rock cross-sections to computed tomography images used for analyzing densities. In one study, advanced techniques in digital imaging were used to analyze geological working faces (Scucka et al., 2006). Image processing was employed by Syamaladevi et al., (2012) to investigate phase transitions on ice recrystallization in Atlantic Salmon during frozen storage. Manahiloh et al., (2018) investigated the effectiveness of threshold-based segmentation in a study that involved muti-phase geomaterials. Imhoff et al., (2017) investigated X-ray CT images to observe how the hydraulic conductivity of a soil varied with biochar addition. Manahiloh and Meehan (2017) used digital image processing to determine the Soil Water Characteristic Curve of a soil. Manahiloh et al., (2016) applied X-ray image-based analysis to perform microstructural investigations on geomaterials.

Image processing could replace the documentation made in the field by hand because it is quicker and more accurate. Taking photos from multiple vantage points creates the opportunity to assemble a three-dimensional (3D) model of the given sample. Applying different shading settings to the images reveals which rock types are present. Image processing is a more economical alternative to more sophisticated methods of analysis. Photogrammetry can also be used to accurately describe rock discontinuities by mapping the physical scale of a sample (Scucka et al., 2006). Algorithms can be used to analyze the geometries in greater detail than manual observations. Soil discontinuities can be found in the pixel intensity changes around

edges, which can be picked up through software algorithms (Deb et al., 2007). Images are taken by placing a camera level with a well-lit rock face and calculating the distance between them using a laser measuring device. Images are typically converted into greyscale before using the edge detection algorithm. The algorithm used by Deb et al. (2007) utilized the fuzzy C-mean clustering and subtractive clustering algorithms. The lighting and camera position are essential factors in generating the amount of error present. Calculations are made to determine the corresponding length of each pixel in the photo using the camera lens size and distance between the specimen and the camera. Clusters of lines are generated on top of the rock edges and sorted for presentation in data tables. The Hough transform removes excessive noise from the photos so that results can remain more accurate (Deb et al., 2007). Removing noise from photos is an important step that reoccurs throughout image processing research. Continuing to develop automated image analysis algorithms will help lead to further improvement in rock mapping methods.

Soil rock mixtures are complicated systems with characteristics that rely on their mesostructures. Digital image processing with finite element analysis techniques can represent geomaterials' inhomogeneities (Xu et al., 2007). Photos are taken of the samples, and noise is removed through digital filtering. Color in the images is converted to grayscale, with each pixel mapped to one of the 256 shades of gray. The pixels are then assigned a unit length for scaling purposes. Major solid rock sections are identified and separated in pre-processing from the soil portion of the sample. The given samples were then sieved to determine whether the image processing of a two-dimensional (2D) sample was accurate. The rock shapes in the cross-section are subject to variability because of how they were cut. After the soil makeup was analyzed, a

shear loading test was simulated on each sample (Xu et al., 2007). It was found that having gravel in the soil improves the soil's shear strength.

These findings were made possible through processing applications that have been recently developed. Digital image processing is a quickly developing field that uses powerful applications such as MATLAB and Java Swing for calculations in geological applications (Shariah et al., 2011). The YUV color space can follow the human perception of color more closely in photo editing. Images are processed before being analyzed so that the visual representation of the data is accurately depicted. Cavities in samples can be identified and measured after they are sharpened and discovered using processing techniques and algorithms (Shariah et al., 2011). Discovering the rock cavities' locations help researchers find potential weak spots in rock samples.

2.2 Image processing in soil mechanics

Image processing can also be a beneficial tool in monitoring soil testing progress by capturing distinct moments during the procedure. The tensile strength of soils is essential but often neglected in testing. Because of increased droughts around the world, learning about soil tensile strength is more critical than it has ever been. A newly designed testing apparatus researched by Li et al. (2019) utilizes image processing during its tensile testing procedure. Pictures were taken every five seconds during the testing to represent the tensile testing visually. Adding water to clayey soil helps its bonding properties between molecules, but once the soil approaches complete saturation, it starts losing a significant amount of strength. The failure occurred in the samples right after peak stress was reached. Test results varied for each sample in this study because the water content directly impacted outcomes (Li et al., 2019). Soil

deformation curves can show the stress-increasing, failure-development, and post-failure stages. The tensile strength is the strongest at the critical water content percentage point. Having images to monitor the testing process is helpful in slow-moving test situations.

Additionally, image analysis is valuable for studying soil crack networks to obtain information about the cracking mechanism and shrinkage during drying (Al-Jeznawi et al., 2020). Soil samples were tested under specific temperatures and pressures to see how they would desiccate. Images were frequently taken during the testing and were then processed to show the cracking results. The results were conveyed through measurements of the crack intensity factor (CIF) and the total crack intensity factor. The friction on the bottom contact surface, the conditions, and the presence of a salt solution affected the crack formation results. In addition, smooth and rough boundaries produced different results. CIF would increase with additional friction on the bottom surface of the samples and when the sample was dried in an open environment. Samples exposed to a salt solution had a lower CIF than those without salt exposure. Tensile stresses significantly affect desiccation cracks in this study (Al-Jeznawi et al., 2020).

Various other studies looked at soil processing from different perspectives. Theocharis et al. (2017) saw soil as consisting of soil particles and voids that a digital fabric can represent. Scan lines were used to distinguish between a sample's soil portions and voids. Discrete element analysis was used to apply a loading path to the scanned 3D fabric, and rattling sections of the scan were removed and treated as voids. Initially, the fabric was isotropic, but during the loading, it gained anisotropy (Theocharis et al., 2017). This method may be used for real cases due to the favorable results. Another study by Charytanowicz and Kulczycki (2015) showed the

process of assembling an image analysis algorithm for soil structure identification. A complete gradient clustering algorithm was built to find pore spaces in the soil. The values of the parameters are calculated using the algorithm, but by changing the values, the results will be altered. A favorable analysis must have the correct smoothing parameter. Photos are taken of the soil, edited, and imported into the computer algorithm system. Three soil samples were dried, sieved, and processed using Aphelion. The software algorithm displayed the pore space with a black filter. Fertilization in the soil resulted in slightly higher pore values than in the control sample (Charytanowicz & Kulczycki, 2015). This new algorithm provided promising results for initial research. Manahiloh et al. (2012) applied image processing to quantify the extent of clogging in pervious concrete.

2.3 X-ray CT Imaging in research

Image processing can also be helpful in academic settings. Learning digital image processing techniques is helpful for students to develop relevant research skills (Aydilek, 2007). Studying the processing methods in-depth helps students understand engineering concepts useful in future studies (Aydilek, 2007). Students must grasp the processing software basics to learn how image processing works. NIH image is another tool that can be used in geological contexts (Bjørnerud & Boyer, 2007). As a free application, it has many built-in functions in commercial image processing packages. Using software with built-in features helps the user to organize and analyze the gathered data more efficiently. Some programs can determine object areas, lengths, and orientations. These functions automate practical tasks like strain analysis, areal estimation, and positioning evaluation. Results can be exported from most software, and 3D models can be constructed. Geotechnical engineering regularly uses centrifuge modeling for research (Zhang et

al., 2008). An image monitoring system was employed to determine soil movement during tests. These images are captured during testing and sent to a computer's memory in the machine. An image-matching algorithm was used to determine the displacement of the soil during the centrifuge test. The movement of each soil point can be tracked through the resulting outputs. The soil failure was found in a shear band less than 1 cm thick (Zhang et al., 2008). The research studies above examined how soil imaging could help analyze soils to quantify characteristics and testing results. Digital images were used to develop results and stimulate findings.

Another form of image analysis can be found in computed tomography (CT). CT scans are stacks of images that depict a substance in three dimensions. X-ray CT data can be used to quantify deformation and strain in soils. In one study by Otani et al. (2020), a triaxial compression test was conducted on the sand, and a digital image correlation was used to see the displacement and strain fields in the soils. CT image stacks are advantageous because more information is available in a 3D model than in a 2D cross-section image. The image is also separated not by the color of the cross-sections but by the density of the objects in the image. The usefulness and accuracy of X-ray CT in geotechnical engineering can be seen in many studies.

X-ray CT can also be used on biocrusts undergoing desiccation (Couradeau et al., 2018). Biocrusts are microbial communities that cover 12% of the earth's continental area. Cyanobacteria produce these crusts by consolidating mineral soil particles through polymeric substances. Biocrusts are only active when wet and spend most of their time in a sleeping desiccated state. The crusts are important for arid ecosystems, and not much was known about them leading up to this research effort. The bacteria stay alive in low-water areas because of their

ability to stay hydrated with the little water input they get. The water interaction with the soil was tested using desiccation methods while quantifying results with X-ray microtomography. The ratios of air, liquid water, and mineral particles were quantified at the microscale. The formation of water gradients showed superior water retention in the bacteria microbes (Couradeau et al., 2018). X-ray is useful for studying all types of soil testing, including desiccation tests for microbial analysis. CT scanning is also helpful in investigating geotechnical properties on a microscopic level (Shan & Lai, 2018). Cracks in soil and rock can be analyzed to find a relationship between the CT number and the level of soil damage. This research conducted a real-time CT experiment that examined uniaxial compression failure. Improving the setting of CT scan parameters can help provide more accurate results for CT testing in geotechnical contexts. Like in other studies, the images gathered were converted into black and white and filtered to sharpen edges and eliminate excess noise. After the images were generated, the pores were identified. The change of gray value in the photo is quantified in different parts of the photo corresponding to the change in pixel values that ranges from 0 to 255 for an 8-bit image. CT image pixels correspond to a CT number that depends on the absorption coefficient of X-rays on the soil sample. White areas map to a high density, while black areas map to a lower density. Different voltages and soils were tested and analyzed using standard deviation to find which sample had the most accurate results. The original data and pixel density are the most important factors for image quality (Shan & Lai, 2018). Adjusting the filtering settings is important for producing images with less noise.

X-ray tomography can also help determine grain-size distributions in geological samples (Safari et al., 2021). The distribution of particle size is used for soil classification, estimation of

hydraulic properties, and evaluation of depositional history. X-ray microcomputed tomography can be used in 2D and 3D contexts to study the geometrical structure of phases in rock samples. The samples were captured using an X-ray radiograph and analyzed using Avizio image processing software. A computer program in Python was developed to process the 2D images, and filters were applied to remove noise. Sandstone was shown to be composed mainly of quartz grains, feldspar, and clay. Porosity was calculated through image processing and standard experimental procedures to see the accuracy of the computer calculations. Pore measurements were close to the computed averages, which showed that this analysis was acceptable (Safari et al., 2021).

Since geotechnical materials are heterogeneous, different parts of the structure have varying responses to external forces. Stress distribution, crack propagation, and failure mode are closely related to material microstructure and heterogeneity (Luo et al., 2019). Finite element modeling can be used to process CT images. The canny operator detects the edges of the image, and pseudo-color enhancement is utilized to enhance the image (Luo et al., 2019). The mesostructure and variation of rock and soil can be analyzed quantitatively. Void distribution influences the mechanical properties of geomaterials. CT scans can be made using medical or industrial X-ray scanners (Ashi, 1997). CT scanning resolution is a precise method of measurement that is useful in discovering the qualities of the test materials. In one study (Ashi, 1997), ocean sediments were analyzed for densities and sample disturbances. Electrical resistivity measurements were also made to determine the porosity after core splitting (Ashi, 1997). CT scans provide an accurate but expensive method of finding sediment densities.

X-ray image analysis has been used to study two-phase flow in porous media to understand the mechanism of nonaqueous light phase liquid migration (Mikami & Mukunoki, 2014). A new test apparatus was developed to measure the flow injection of micro-focused X-ray CT scanners. Pore structures in the soils were evaluated through cluster analysis (Mikami & Mukunoki, 2014). The water content in the soil can be found through the oven baking method, which measures the weight of the soil sample before and after cooking it in an oven to dry it out completely.

Flow details in porous soil can be improved by analyzing CT scans of wet and dry soil samples (Heijs & Lange, 1997). Test phantoms determined the optimal scanner settings to get images with a bimodal gray value distribution with high contrast and a low standard deviation. The high contrast between the pores and the clay allowed thresholding for the separation, where the connectivity and topology of the pore networks were preserved. The water content distribution was determined by contrasting the dry and wet samples of soil. Water flow through pore networks was more easily found through CT scanning methods (Heijs & Lange, 1997). Water content in clay soil was also analyzed using CT to see if it could be used as a filling material for freeway embankments (Zhang et al., 2015). Moisture migration was monitored in soils of different levels of compaction. The testing showed that the groundwater level and the degree of compaction significantly affected the moisture migration rate (Zhang et al., 2015).

These studies showed how image analysis of soils could be useful in finding water flow, porosity, and many other qualities. CT scans are a helpful tool that accurately depicts soil samples in 3D space. Though many studies have looked at how image processing can be used in geotechnical applications, there is a need to find the phase ratios of water, solids, and air through

nondestructive X-ray analysis. The phase quantities will be found and analyzed in a CT capture of a soil sample through the Image-Pro Premier® processing tool.

Chapter 3

INVESTIGATION OF X-RAY CT IMAGES

3.1 X-ray CT

The testing begins with the gathering of images from an industrial CT scanner. The sample was placed in a Tempe Pressure Cell with a diameter of 10 millimeters. The pressure in the cell regulates the amount of water that stays in the sample at a given time. In this case, the hanging water column technique was applied to monitor the suction level inside the Tempe Cell. The cell can be seen in Figure 1.

Figure 1

Tempe Pressure Cell

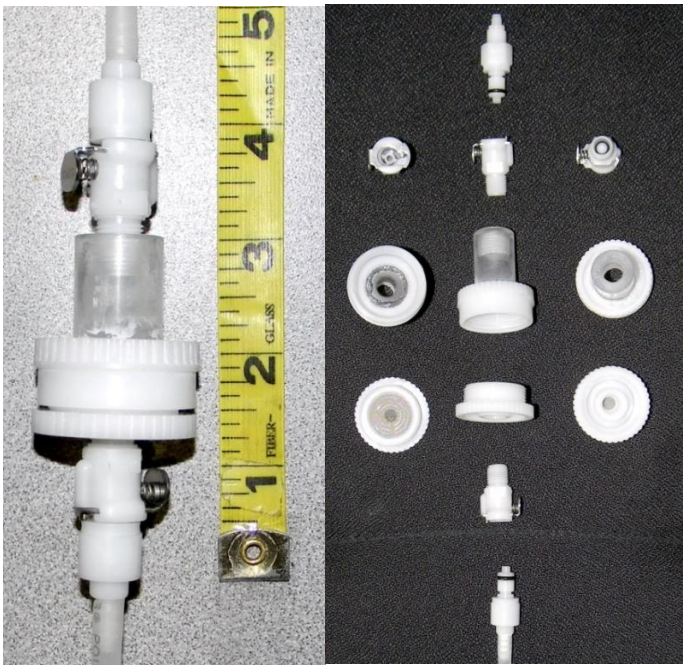

Note. Image used with permission. From Manahiloh, K. N. (2013). Microstructural analysis of unsaturated granular soils using x-ray computed tomography. (Publication No. 3598095) [Doctoral dissertation, Washington State University]. ProQuest Dissertations and Theses Global.

The six samples were prepared from a mixture of different size glass beads, water, and air. Each sample image represents the average cross-section of the sample at a specific suction pressure value on either the wetting or the drying curve. The same analysis completed on these individual slices of a 3D photo stack can be applied to stacks of hundreds to thousands of photos. A virtual 3D sample constructed from stacks of 2D X-ray images can be seen in the bottom right portion of Figure 2.

Figure 2

Isometric and 3D views of an image sequence

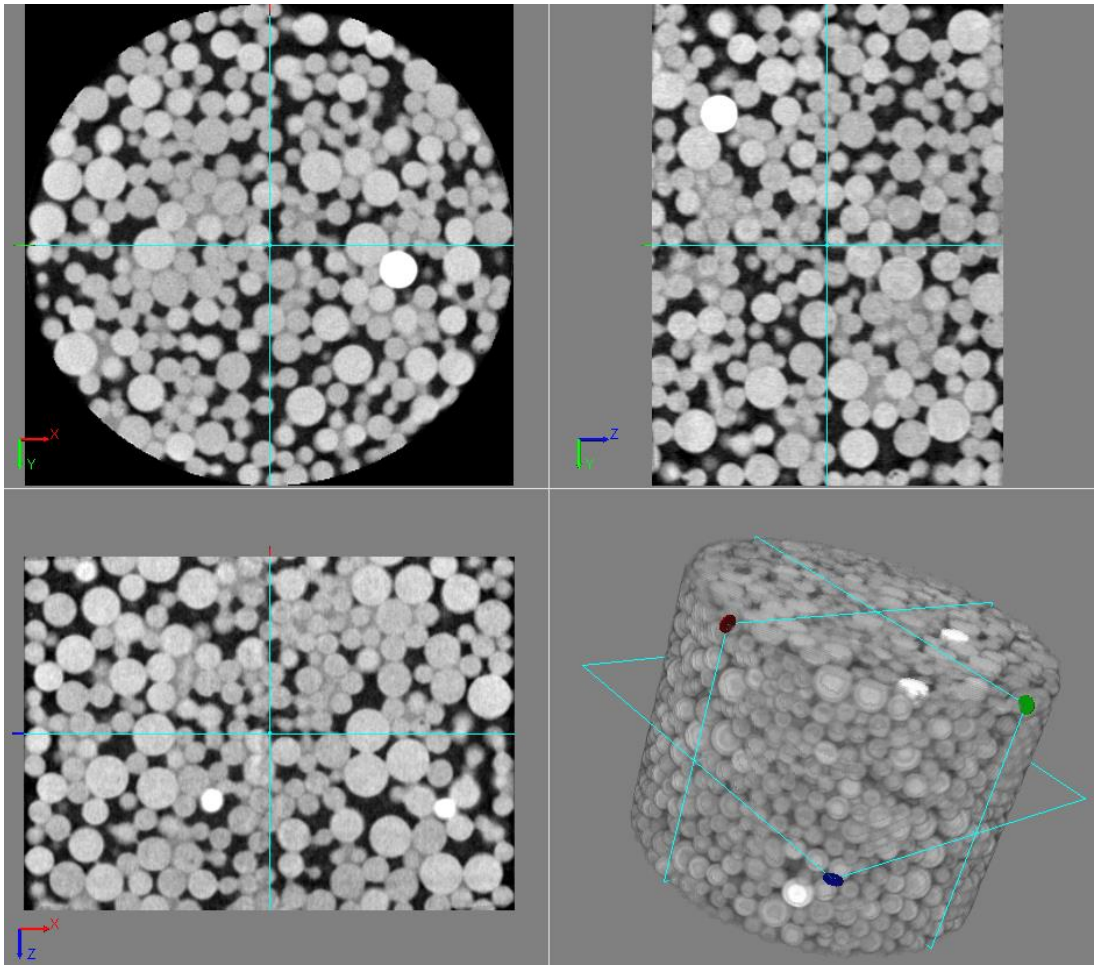

Having all three soil phases in the sample is vital to the computational section of the study. The 2D sample images used from the scan before processing can be seen in Figure 3.

Figure 3

Initial six sample images, samples numbered 1-6

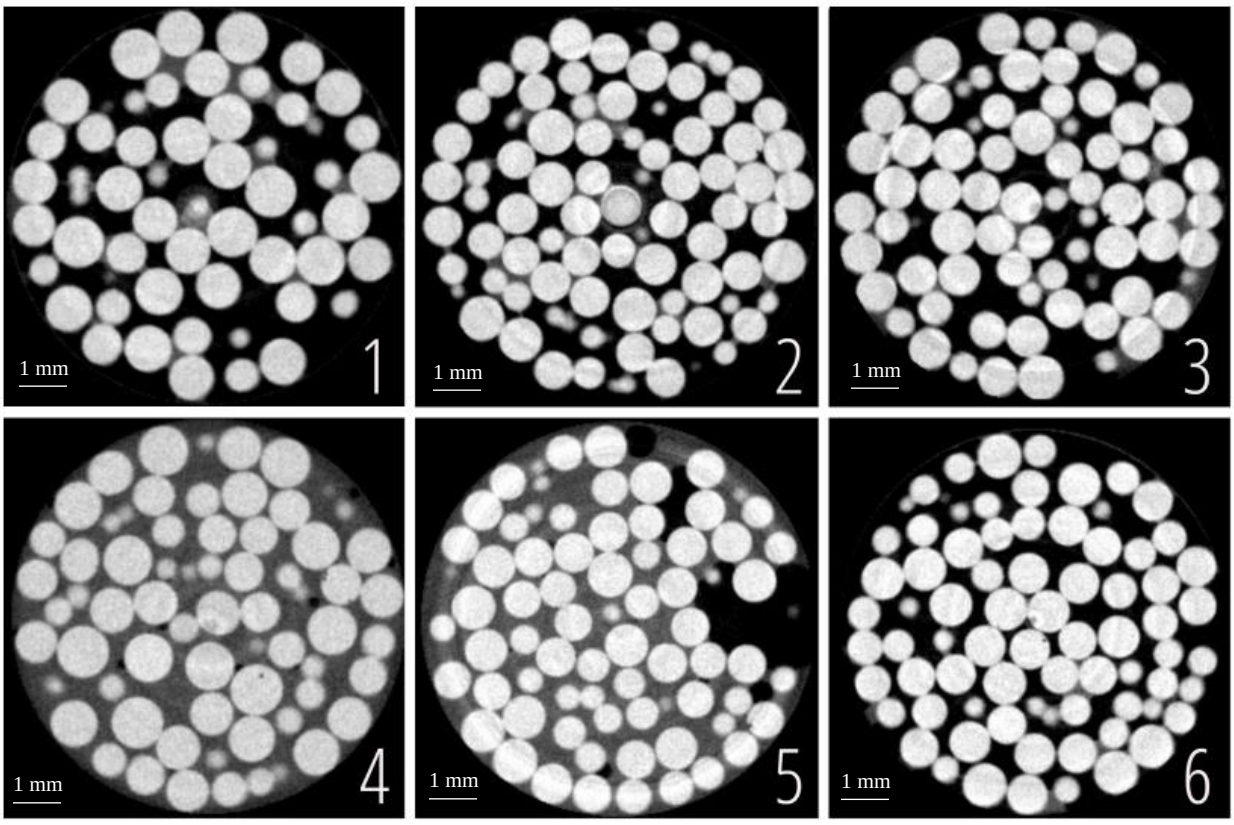

In the images, the bright pixels represent the glass beads, while the grays correspond to the water, and the black matches the gas phases in the granular media. Initially, the plan was to process a 3D stack of over 1,000 photos. However, due to the timeline, available computing power, and software permissions, a 2D analysis of six sample slices was selected for processing and analysis.

Each of the six samples was taken from a specific location in the Soil Water Characteristic Curve (SWCC). These specific locations were chosen at 0, 0.6, and 1.8 kPa on the wetting (1-3)

or the drying (4-6) curve of the soil water characteristic curve (SWCC). The SWCC shows the relationship between the suction pressure and the degree of saturation (water content) in soil. The SWCC is inherently hysteretic and won't travel the same path as the soil specimen gets wet and dry. The SWCC of the examined glass bead specimen is shown in Figure 4.

Figure 4

Soil water characteristic curve of the examined specimen

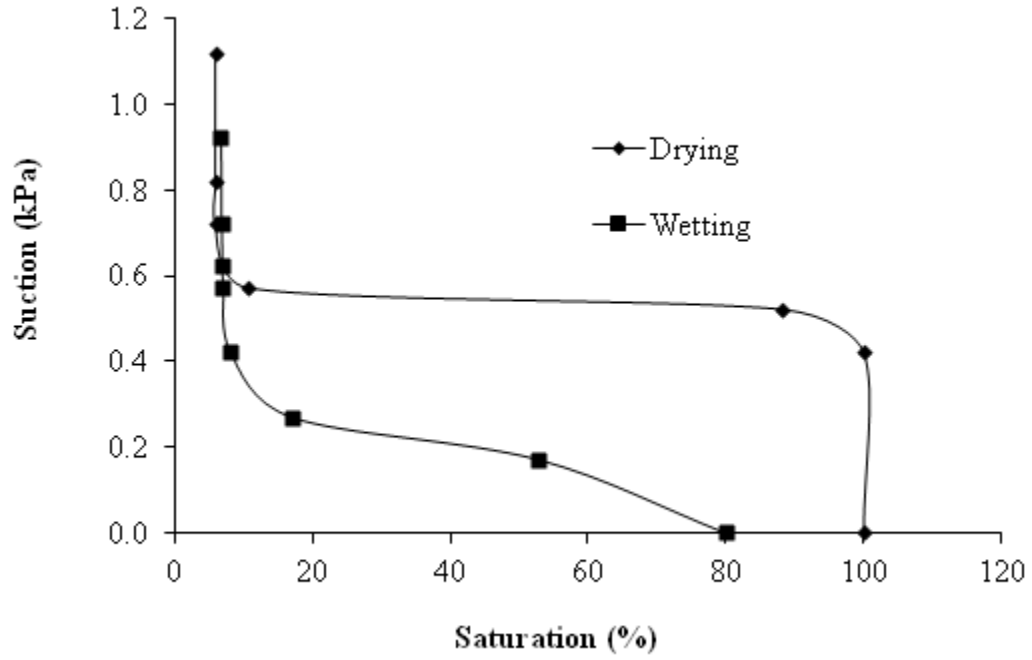

3.2 Image Processing

The image processing tool selected for this research work is Image-Pro Premier® version 9.2. This software offers many built-in settings for image editing and can input coding for specific analyses not included in its basic functioning. These coding macros can perform many different specialized tasks that benefit analysis.

Once the images have been gathered, they need to be edited and filtered so that the separation code will accurately portray reality. The first step in the editing process in Image-Pro Premier® is to crop the photo of the specimen so that it only includes the informative portion of the picture. Cropping can be done using the regions of interest selection tool to pick out the appropriate portion of the object in the picture, as seen in Figure 5, by hitting the crop button to paste that section onto a new image below the image strip.

Figure 5

Image-Pro Premier® circular cropping tool

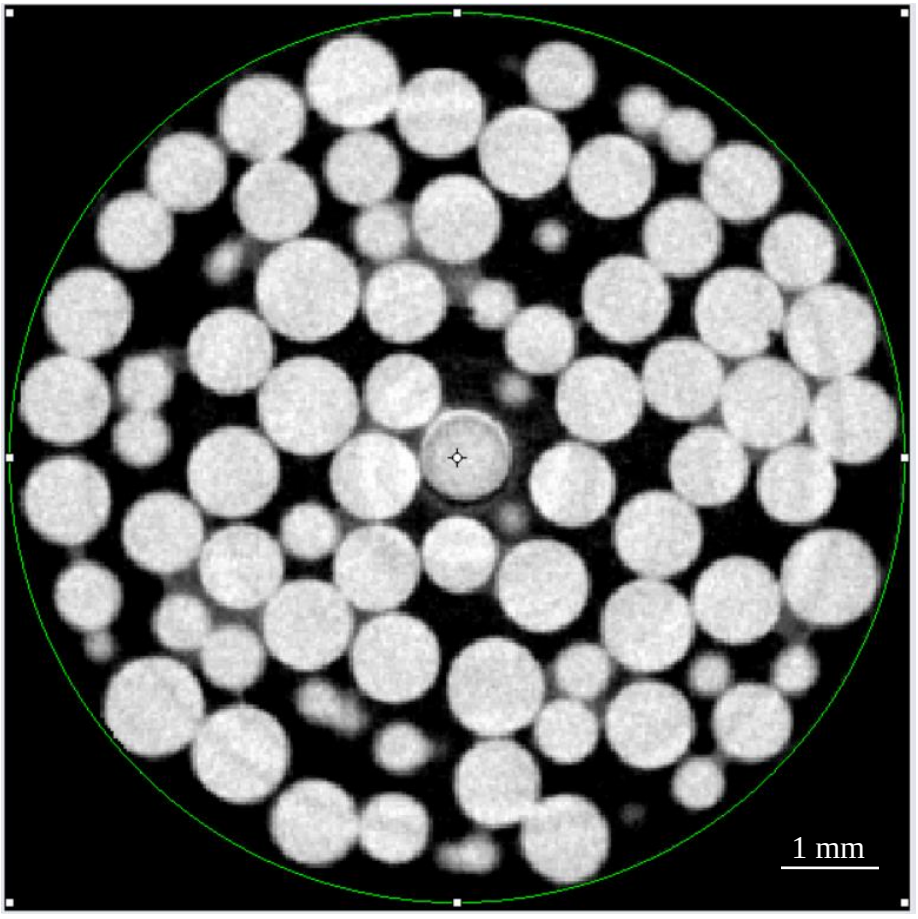

Next, the image area and pixel size are determined by assigning the picture length to the appropriate distance in the program. This calibration process changes values from pixels squared

into the unit selected for analysis. In this study, each sample was matched to its 10-millimeter diameter of the Tempe Cell.

Six different sample photos were analyzed in this study to see if the three phases of soil could be separated and quantified through image processing. The 2D analysis of each cross-section started with trying out different filtering techniques to adjust the given photos. After trying all the filters, they changed the original data instead of accurately portraying the given scans. Therefore, this original editing batch did not use the image enhancement tool. After the images were cropped using the regions of interest tool, they were separated into phases using the innovative segmentation feature of Image-Pro Premier®. The first step was to select the objects on the photo with high-density white shading using the draw objects selection on the smart segmentation tab, see Figure 6.

Figure 6

Object selection using the smart segmentation drawing tool

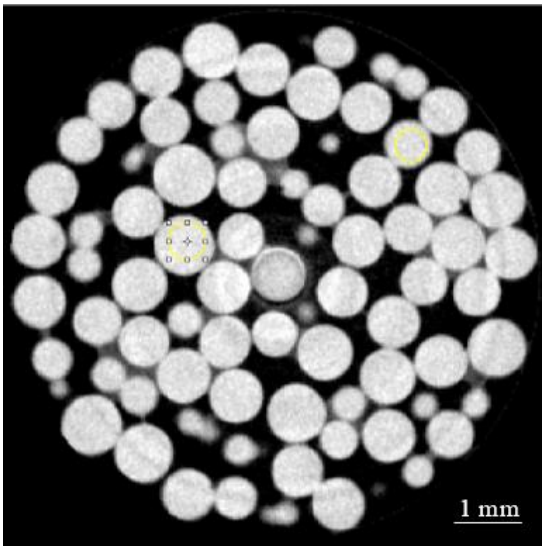

After many similar objects are selected, a background is specified by selecting the low-density black spaces on the scan corresponding to the air phase. Once the background is

specified, the smart segmentation will assign new pixel colors according to the selected color for the object and background in the smart segmentation tab. The selected solids can be seen in yellow, while the background is dark black (see Figure 7).

Figure 7

Singly segmented image, solids in yellow, voids in grey and black

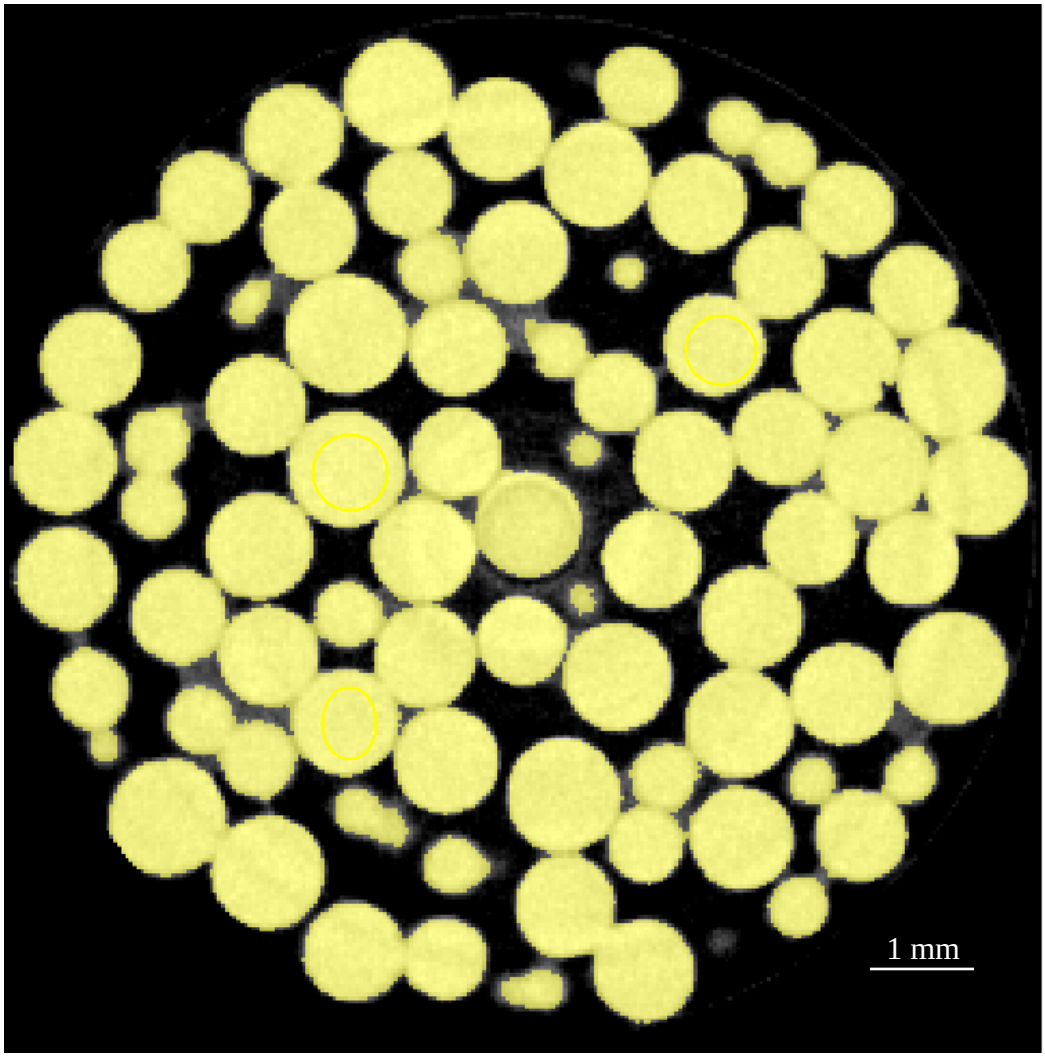

Since this research consists of 3 phases, another selection must be made—this time, the smart segmentation is set to class 2, differentiating between previous selections. In addition, this assigns a different coloring to the specified pixel range. The water sections of the samples were

selected and given a shade of blue to show the saturation. The same air background was selected and kept black so that the value of the solids would stay yellow. The completed segmentation can be seen in Figure 8.

Figure 8

Three-phase segmented images

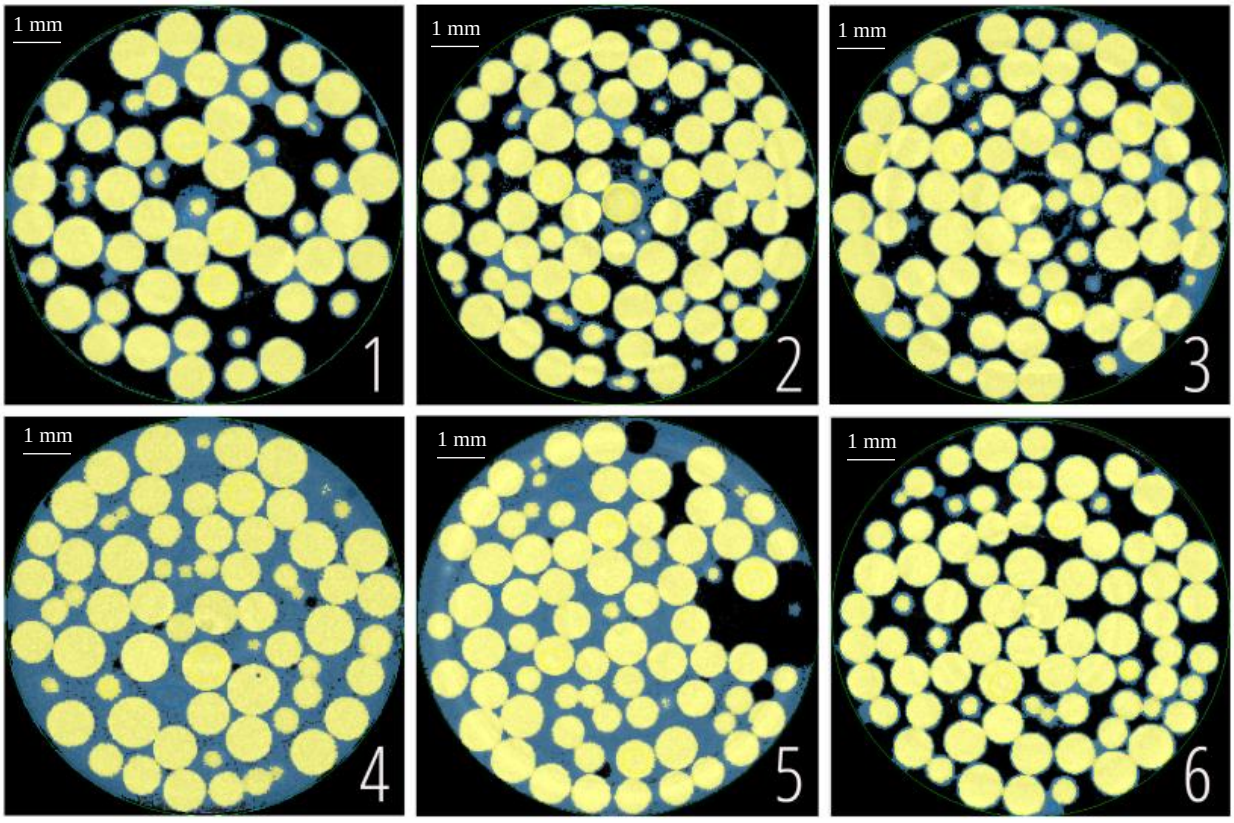

While the accuracy of the backing algorithm for this function was very adept, it still was not always perfect in usage. While using the original photo as a reference, area selections were made in reaction to the initial results until the desired outcome was achieved. This process was not exceedingly time-consuming nor challenging to accomplish. However, the user should select areas for smart segmentation in a careful manner to deliver accurate results. The color and background tabs in smart segmentation should be turned on so that the picture displays the

desired pixel coloring. Following the segmentation, the count function should be used to find the total area in square millimeters for each phase. By selecting the table tab, the results can be seen at the bottom of the screen in Image-Pro Premier®. After the image is divided into sections, the pixel count information can be exported into Excel for further analysis.

Chapter 4

RESULTS AND DISCUSSION

The three-phase segmentation was successful in each of the three images analyzed. The solids, water, and air were rendered yellow, blue, and black, respectively. After each image is cropped by drawing a circular region of interest (ROI), calculations were made for each ROI to find the total area occupied by pixels of similar gray value. The pixel dimensions of the images are converted into their equivalent areas in mm^2 by applying calibration factors. The following equation for finding the area of a circle was used.

$$A = \pi r^2 \quad (1)$$

The calculations for each circular area in square millimeters are as follows.

$$Sample\ Area = \pi * 5\ mm * 5\ mm = 78.54\ mm^2 \quad (2)$$

Table 1 shows the areas occupied by each phase for each sample.

Table 1

Calculated phase percentages

	Sample 1	Sample 2	Sample 3	Sample 4	Sample 5	Sample 6
Total Area (mm^2)	78.54	78.54	78.54	78.54	78.54	78.54
Solid Area (mm^2)	39.15	45.49	45.04	46.44	43.40	44.80
Solid Area %	49.85%	57.92%	57.35%	59.13%	55.26%	57.04%
Water Area (mm^2)	14.34	10.40	14.11	30.26	26.59	10.76
Water Phase %	18.26%	13.24%	17.97%	38.53%	33.86%	13.70%
Air Area (mm^2)	25.05	22.66	19.39	1.84	8.55	22.98
Air Phase %	31.89%	28.85%	24.69%	2.34%	10.89%	29.26%

Although the photos differed in pixel counts, the calibration evened the area calculation between samples. As can be expected from seeing the sample images, the solid phase occupied the most space across the images, while the air had a greater area than the water phase did across the

board. The solid area results were exported to Excel and added together using the sum function for each data table. Likewise, the water area in class 2 was exported to Excel and then summed for its area totals. The air phase was found by subtracting the water and solid areas from the total area of each sample to find the total black space in each image. The phase percentages were calculated by using the following equation.

$$Phase\ Percentage = \frac{Phase\ Area}{Total\ Area} * 100\% \quad (3)$$

The phase percentage results for each sample were then inserted into Figure 9.

Figure 9

Phase proportioning bar graph

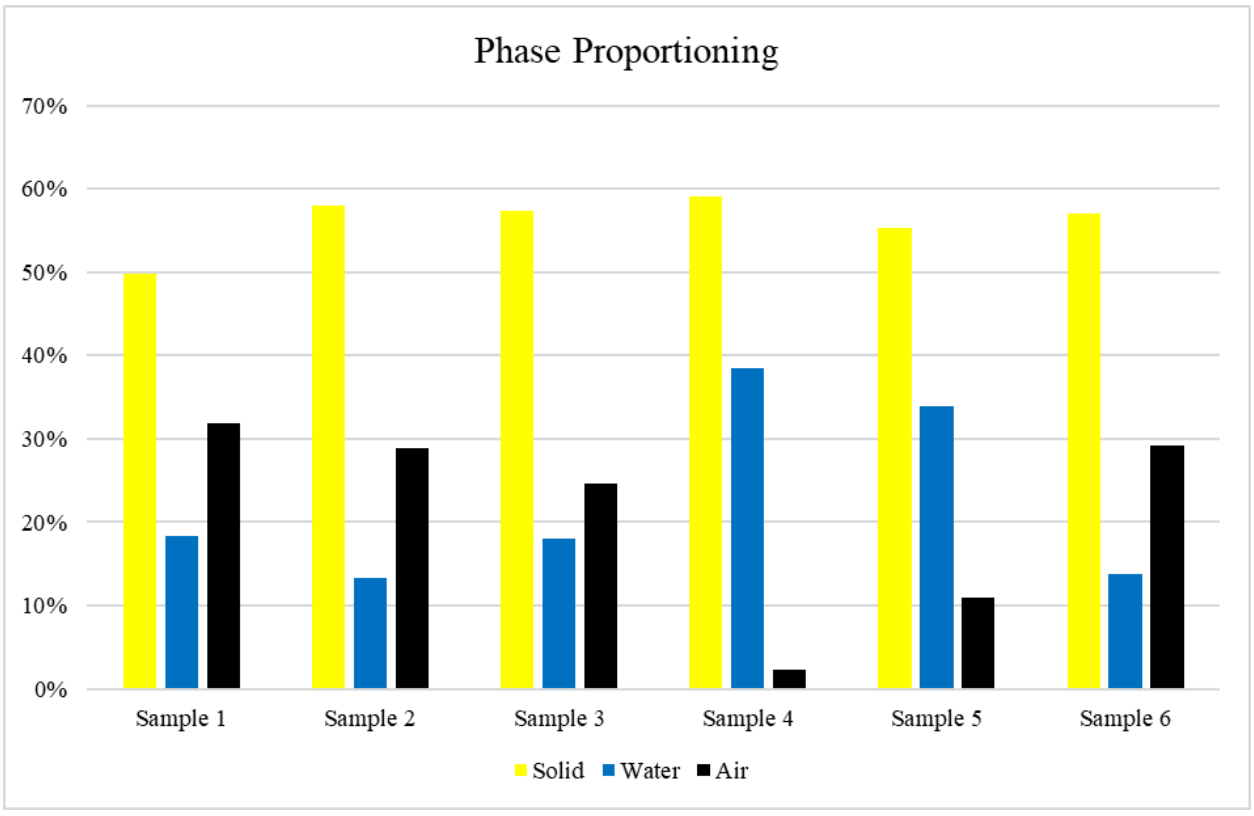

Sample Calculations

Obtaining the phase quantities can help determine other valuable calculations by applying phase relationships. One value that can be calculated from areal ratios is the void ratio (e). For these sample calculations, the phase quantities of sample 1 will be used. Since the analyzed images are 2D cross-sections, the average thickness of the three samples is assumed to be equal. Thus, the average areas for each phase will be used instead of the volume in the void ratio calculation.

$$e = \frac{V_v}{V_s} = \frac{V_v}{V_s} * \frac{thickness}{thickness} = \frac{A_v}{A_s} = \frac{area(Air+Water)}{area(Solids)} \quad (4)$$

$$e = \frac{25.05+14.34}{39.15} = 1.006 \quad (5)$$

The porosity (n) can also be calculated using the area of the voids and the total area of the sample.

$$n = \frac{V_v}{V_t} * 100\% = \frac{V_v}{V_t} * \frac{thickenss}{thickness} = \frac{A_v}{A_t} = \frac{area(Air+Water)}{Total\ Area} \quad (6)$$

$$n = \frac{25.05+14.34}{78.54} * 100\% = 50.15\% \quad (7)$$

Similarly, the degree of saturation (S) can be found by dividing the average area of water by the average area of voids as follows.

$$S = \frac{V_w}{V_v} * 100\% = \frac{V_w}{V_v} * \frac{thickness}{thickness} = \frac{A_w}{A_v} = \frac{area(Water)}{area(Water+Air)} \quad (8)$$

$$S = \frac{14.34}{14.34+25.05} * 100\% = 36.41\% \quad (9)$$

To find the moisture content (*w*) of the average sample, a specific gravity of 2.5 will be used for the glass beads in the cross-section. A depth of 1 mm will be used in the equation with the knowledge that the millimeters will cancel out.

$$w = \frac{M_w}{M_s} * 100\% = \frac{\rho_w * V_w}{\rho_s * V_s} * \frac{thickness}{thickness} * 100\% \quad (10)$$

$$w = \frac{\frac{0.001g}{mm^3} * 14.34\ mm^2}{\frac{0.0025g}{mm^3} * 39.15\ mm^2} * 100\% = 14.65\% \quad (11)$$

The moisture content is helpful in finding the specific weight of the whole sample.

$$\gamma_m = \gamma_d(1 + w) = \frac{9810 * 2.5 * 39.15N}{78.54\ m^3} * (1 + 0.1465) = 14{,}016\ N/m^3 \quad (12)$$

This is done by taking the dry unit weight and multiplying it by one plus the moisture content value. The moisture content ratio accounts for the amount of water in the whole sample based on weight. The specific gravity of the material can be determined with the total unit weight found.

$$G_m = \frac{\gamma_m}{\gamma_w} = \frac{14016}{9810} = 1.43 \quad (13)$$

The void ratio can be calculated using other variables.

$$e = \frac{G_s \gamma_w}{\gamma_d} - 1 = \frac{2.5 * 9810}{12225} - 1 = 1.006 \quad (14)$$

Another relationship among variables that can be used to confirm the calculated values is:

$$G_s w = Se \Leftrightarrow 2.5 * 0.1465 = 0.3641 * 1.006 = 0.3663 \quad (15)$$

The same calculations were made for samples 2 through 6 and can be seen in Table 2.

Table 2

Calculated values for all samples

Value	Sample 1	Sample 2	Sample 3	Sample 4	Sample 5	Sample 6
e	1.006	0.727	0.744	0.691	0.810	0.753
n	50.15%	42.09%	42.65%	40.87%	44.74%	42.96%
S	36.41%	31.46%	42.12%	94.27%	75.67%	31.89%
w	14.65%	9.14%	12.53%	26.06%	24.51%	9.61%
γ_d *(N/m^3)*	12225	14205	14064	14501	13552	13989
γ_m *(N/m^3)*	14016	15504	15827	18281	16873	15333
G_m	1.43	1.58	1.61	1.86	1.72	1.56

The calculated results show that the void ratio, porosity, and degree of saturation can be determined through 2D CT analysis. Finding the specific gravity of the solid phase opens other soil mechanic equations to discover more attributes of the given sample. The results found from this X-ray analysis are an accurate representation of the soil phase makeup. This form of analysis could prove to be helpful in future research.

Chapter 5

CONCLUSIONS & RECOMMENDATIONS

In this study, digital image processing was shown to be a useful method to investigate granular media. X-ray CT images of a partially saturated granular media were analyzed with Image-Pro-Premier®. Results showed that as suction increases, the amount of water in the sample decreased. This was verified from image-based results that were calculated as part of this thesis. The application areas of image processing were highlighted in this thesis. Image-Pro Premier® was shown to be an elegant tool that can be used for image enhancement, segmentation, and pixel counting.

Many factors could be added to this research to continue advances. Analyzing different soil types and particles to see if the same success in segmentation can be found for more difficult-to-process images is one step that could be implemented. Another factor that would be informative is to see if it is possible to calculate the density of the solids by using the CT pixel ratings and test how accurate specific gravity calculations can be. Experimenting with saturated clay would be interesting as that soil bonds to water, making image analysis challenging. The test sample used in this research was only one centimeter in diameter. Would using a larger sample be helpful or create problems? Lastly, researching a complete 3D specimen could be more informative on specific samples given the necessary computing power and could be worth investigating. Soil is all around us, and the ratio of its phases is more critical than most people recognize. Finding new and improved ways of analyzing soil is essential to the future of geotechnical studies and is worth the time investment of those undertaking such research.

REFERENCES

Al-Jeznawi, D., Sanchez, M., & Al-Taie, A. J. (2020). Using image analysis technique to study the effect of boundary and environment conditions on soil cracking mechanism - geotechnical and geological engineering. *Geotechnical and Geological Engineering, 39,* 25-36. https://doi.org/10.1007/s10706-020-01376-5

Ashi, J. (1997). Computed tomography scan image analysis of sediments. *Proceedings of the Ocean Drilling Program, Scientific Results, 156,* 151-159. http://www-odp.tamu.edu/publications/156_SR/11_CHP.PDF

Aydilek, A. H. (2007). Digital image analysis in geotechnical engineering education. *Journal of Professional Issues in Engineering Education and Practice, 133,* 38-42. https://doi.org/10.1061/(ASCE)1052-3928(2007)133:1(38)

Bjørnerud, M. G., & Boyer, B. (2007). Image analysis in structural geology using NIH image. *Computer Methods in the Geosciences, 15,* 105-121. https://doi.org/10.1016/S1874-561X(96)80012-5

Charytanowicz, M., & Kulczycki, P. (2015). An image analysis algorithm for soil structure identification. *Advances in Intelligent Systems and Computing, 323,* 681-692. https://doi.org/10.1007/978-3-319-11310-4_59

Couradeau, E., Felde, V. J. M. N. L., Parkinson, D., Uteau, D., Rochet, A., Cuellar, C., Winegar, G., Peth, S., Northen, T. R., & Garcia-Pichel, F. (2018). In situ X-ray tomography imaging of soil water and cyanobacteria from biological soil crusts undergoing desiccation. *Frontiers in Environmental Science, 6*(65), 1-11. https://doi.org/10.3389/fenvs.2018.00065

Deb, D., Hariharan, S., Rao, U. M., & Ryu, C.-H. (2007). Automatic detection and analysis of discontinuity geometry of rock mass from Digital Images. *Computers & Geosciences, 34,* 115-126. https://doi.org/10.1016/j.cageo.2007.03.007

Heijs, A., & Lange, J. (1997). Determination of pore networks and water content distributions from 3-D computed tomography images of a clay soil. *Bioimaging, 5,* 194-204. https://doi.org/10.1002/1361-6374(199712)5:4<194::AID-BIO3>3.0.CO;2-3

Imhoff, P. T., Nakhli, S. A. A., Mills, G., Yudi, Y., Abera, K., Williams, R., Manahiloh, K. N., & Willson, C. S. (2017). X-ray computed tomography and pore network modeling to assess the impact of biochar on saturated hydraulic conductivity of stormwater infiltration media. *AGU Fall Meeting Abstracts 2017*, H43Q-06

Li, H.-D., Tang, C.-S., Cheng, Q., Li, S.-J., Gong, X.-P., & Shi, B. (2019). Tensile strength of clayey soil and the strain analysis based on image processing techniques. *Engineering Geology, 253,* 137-148. https://doi.org/10.1016/j.enggeo.2019.03.017

Luo, G., Pan, S., Zhang, Y., Jia, H., & Chen, L. (2019). Research on establishing numerical model of GEO material based on CT image analysis. *EURASIP Journal on Image and Video Processing, 36,* 1-11. https://doi.org/10.1186/s13640-019-0421-z

Manahiloh, K. N. (2013). Microstructural analysis of unsaturated granular soils using x-ray computed tomography. (Publication No. 3598095) [Doctoral dissertation, Washington State University]. ProQuest Dissertations and Theses Global.

Manahiloh, K. N., Abera, K., & Motalleb Nejad, M. (2018). A refined global segmentation of x-ray CT image for multi-phase geomaterials. *Journal of Nondestructive Evaluation, 37,*54. https://doi.org/10.1007/s10921-018-0508-y

Manahiloh, K. N., & Meehan, C. (2017). Determining the soil water characteristic curve and interfacial contact angle from microstructural analysis of x-ray CT images. *Journal of Geotechnical and Geoenvironmental Engineering, 143,* 8. https://doi.org/10.1061/(ASCE)GT.1943-5606.0001677

Manahiloh, K. N., Muhunthan, B., Kayhanian, M., & Gebremariam, S. (2012). X-Ray Computed Tomography and Nondestructive Evaluation of Clogging in Porous Concrete Field Samples. *Journal of Materials in Civil Engineering, 24,* 8. http://dx.doi.org/10.1061/(ASCE)MT.1943-5533.0000484

Manahiloh, K. N., Muhunthan, B., & Likos, W. (2016). Microstructure-based effective stress formulation for unsaturated granular soils. *International Journal of Geomechanics, 16,* 6. http://doi.org/10.1061/(ASCE)GM.1943-5622.0000617

Mikami, K. & Mukunoki, T. (2014). Study on mechanism of two-phase flow in porous media using micro focused x-ray CT. *International Petroleum Technology Conference.* https://doi.org/10.2523/IPTC-17676-MS

Otani, J., Watanabe, Y., & Chevalier, B. (2020). Introduction of x-ray CT application in geotechnical engineering – theory and practice. *IOP Conference Series: Materials Science and Engineering, 10,* 1-10. https://doi.org/10.1088/1757-899X/10/1/012089

Safari, H., Balcom, B. J., & Afrough, A. (2021). Characterization of pore and grain size distributions in porous geological samples – an image processing workflow. *Computers & Geosciences, 156,* 1-14. https://doi.org/10.1016/j.cageo.2021.104895

Scucka, J., Martinec, P., Snuparek, R., & Vesely, V. (2006). Image processing and analysis in geotechnical investigation. *Tunneling and Underground Space Technology, 21,* 223. https://doi.org/10.1016/j.tust.2005.12.005

Shan, P., & Lai, X. (2018). Influence of CT scanning parameters on rock and soil images. *Journal of Visual Communication and Image Representation, 58,* 642-650. https://doi.org/10.1016/j.jvcir.2018.12.014

Shariah, M. A., Shariah, S.K., Samsudin, & Ramli, A.R. (2011). Image processing for geological applications. *NGC 2011: Geoscientists and Ethics for a Sustainable Society,* 150-151. https://www.researchgate.net/publication/256813486_Image_processing_for_geological_applications

Syamaladevi, R., Manahiloh, K. N., Muhunthan, B., & Sablani, S. (2012). Understanding the influence of state/phase transitions on ice recrystallization in atlantic salmon (*salmo salar*) during frozen storage. *Food Biophysics, 7,* 57-71. https://doi.org/10.1007/s11483-011-9243-y

Theocharis, A. I., Vairaktaris, E., & Dafalias, Y. F. (2017). 3D scan line method for identifying void fabric of granular materials. *EPJ Web of Conferences, 140,* 1-4. https://doi.org/10.1051/epjconf/201714012021

Xu, W., Yue, Z., & Hu, R. (2007). Study on the mesostructure and mesomechanical characteristics of the soil–rock mixture using digital image processing based finite element method. *International Journal of Rock Mechanics and Mining Sciences, 45,* 749-762. https://doi.org/10.1016/j.ijrmms.2007.09.003

Zhang, G., Hu, Y., & Zhang, J. (2008). New image analysis-based displacement-measurement system for geotechnical centrifuge modeling tests. *Measurement, 42,* 87-96. https://doi.org/10.1016/j.measurement.2008.04.002

Zhang, J., Jiang, Q., Zhang, Y., Dai, L., & Wu, H. (2015). Nondestructive measurement of water content and moisture migration of unsaturated red clays in South China. *Advances in Materials Science and Engineering, 2015,* 1-7. https://doi.org/10.1155/2015/542538